Mathematics

http://www.aimspress.com/journal/Math

AIMS Mathematics, 11(6): 18553–18579.
DOI: 10.3934/math.2026754
Received: 17 March 2026
Revised: 01 June 2026
Accepted: 12 June 2026
Published: 24 June 2026

Research article

Memory and delayed investment response in a Caputo fractional financial system: stability, transient dynamics, and residual-verified computation

Alvaro H. Salas[1,*], **Gilder Cieza Altamirano**[2,3] **and Lorenzo Julio Martínez Hernández**[4,5]

[1] FIZMAKO Research Group, Department of Mathematics and Statistics, Universidad Nacional de Colombia, Sede Manizales, Manizales, Colombia

[2] Universidad Nacional Autónoma de Chota, Cajamarca, Perú; gciezaa@unach.edu.pe

[3] FIZMAKO Research Group, Colombia

[4] Universidad Nacional de Colombia, Manizales, Colombia

[5] Universidad de Caldas, Manizales, Colombia

* **Correspondence:** Email: ahsalass@unal.edu.co.

Abstract: This paper studies the effect of memory and delayed investment response in a Caputo fractional version of the Chen financial system. The model describes the interaction between the interest rate, investment demand, and price index through a three-dimensional fractional delay system. Two mechanisms are incorporated simultaneously: a Caputo derivative of order $0 < \rho < 1$, which represents hereditary memory, and a discrete delay in the nonlinear investment feedback, which models the fact that investment decisions do not react instantaneously to previous market conditions.

The equilibrium points of the system are obtained explicitly. The local stability problem is then formulated through the characteristic equation of the linearized fractional delay system. For the equilibrium E_0, a corrected stability condition is derived in terms of the fractional stability criterion. For the nontrivial equilibria $E_{\pm}$, where the delay enters the characteristic equation explicitly, a numerical crossing procedure is used to identify delay-dependent stability changes. This provides a concrete way to examine how the fractional order and the delay parameter influence the response near equilibrium.

The numerical dynamics are computed by a predictor-corrector method adapted to Caputo fractional delay equations. To strengthen the reliability of the simulations, the computed trajectories are verified by an independent residual diagnostic based on a quintic Caputo reconstruction. The numerical study is organized around the separate and combined effects of memory and delay. Variations of the fractional order show that memory can modify the amplitude, duration, and smoothing of transient excursions. Variations of the delay show that lagged investment feedback can shift and amplify the transient response. Additional comparisons between delayed and nondelayed dynamics, as well as between fractional and integer-order responses, clarify the distinct roles of these two mechanisms.

The results indicate that delayed investment response and fractional memory act in different directions in the organization of the financial dynamics. The delay tends to promote transient amplification and phase shifting, whereas fractional memory can moderate or postpone these effects. The study is therefore presented as a stability-oriented and residual-verified numerical analysis of a delayed fractional financial model. It does not claim a complete bifurcation or chaos classification; rather, it provides a reproducible framework and identifies Lyapunov-exponent computation, continuation analysis, and broader parameter exploration as natural directions for future work.

Keywords: Caputo derivative; fractional financial system; delayed investment response; fractional delay differential equations; local stability; transient dynamics; predictor-corrector method; residual verification; memory effects
Mathematics Subject Classification: 34A08, 34K37, 37N40, 65L05, 65L20

1. Introduction

Nonlinear financial models provide a useful mathematical framework for understanding the emergence of endogenous oscillations, instability, and complex responses in interacting economic variables. In contrast with purely linear descriptions, nonlinear systems can represent feedback mechanisms, saturation effects, delayed adjustment, and the sensitivity of market variables to previous states. Such mechanisms are important because financial systems are rarely governed by instantaneous and proportional responses alone. Interest rates, investment demand, and price indices interact through feedback loops that may generate transient amplification, persistent oscillation, or even irregular dynamics under suitable parameter regimes [1, 2, 6].

The model studied in this paper belongs to the family of nonlinear finance systems initiated by Ma and Chen and subsequently investigated in integer-order, delayed, and fractional forms [1, 5, 6]. In the classical formulation, the variables usually represent the interest rate, investment demand, and price index. The interaction among these variables leads to a three-dimensional nonlinear system whose qualitative behavior depends strongly on the balance between feedback, dissipation, and external economic input. Later studies showed that the model and its variants can display Hopf bifurcations, delayed-feedback effects, and chaotic or hyperchaotic regimes under suitable conditions [6–8].

Fractional calculus has become a natural tool for extending such models because economic and financial processes often display memory, persistence, and hereditary dependence. A fractional derivative does not only measure an instantaneous rate of change; it incorporates a history-dependent convolution kernel. This feature is particularly meaningful in economic modeling, where current decisions may be influenced by accumulated market information, previous interest-rate regimes, delayed expectations, and the persistence of investment trends. The Caputo derivative is especially convenient for initial-value problems because it permits classical initial data while preserving the nonlocal memory structure [12, 14, 15]. Fractional economic modeling has also been discussed from a broader methodological perspective in the literature on fractional economics [4].

Time delay is another central mechanism in economic dynamics. Investment decisions are rarely adjusted immediately after a change in the interest rate or market conditions. Delays can arise from information processing, institutional decision times, policy implementation, credit restrictions, expectation formation, and the time required for firms to modify investment plans. In nonlinear models, such lags may have a strong destabilizing influence. Even if the equilibrium coordinates are unchanged by a constant delay, the linearized perturbation equations may acquire exponential delay factors that alter the spectrum and may produce stability switches or oscillatory responses [6, 8, 9].

The simultaneous presence of fractional memory and explicit delay creates a richer modeling structure. The fractional derivative represents distributed memory over the entire past, while the discrete delay represents a particular response lag in a selected feedback channel. Recent studies on fractional-order financial systems with time delays have shown that these two ingredients can substantially change the organization of the dynamics, including complexity measures, bifurcation diagrams, and stability properties [8, 10]. Related work on multistable fractional-order systems also emphasizes that fractional order and coupling mechanisms can strongly modify attractor selection and transient behavior [11]. More broadly, reviews in social physics highlight the importance of mathematical models that combine nonlinear interaction, memory, networked response, and delayed adaptation in social and economic systems [3].

The present paper focuses on a Caputo fractional delayed variant of the Chen financial system. The extension is intentionally modest and specific: The classical fractional financial system is modified by inserting a single discrete delay into the nonlinear squared-interest-rate feedback in the investment equation. This means that the model should be interpreted as a focused delayed variant of an existing financial system, not as an entirely new financial model. The delayed term is placed in the nonlinear investment-feedback channel because the inhibitory effect of borrowing conditions on investment demand is not instantaneous in realistic markets. The current damping term in the investment equation is left nondelayed because it represents an immediate relaxation tendency, whereas the squared interest-rate feedback is interpreted as the delayed effect of previously observed financial pressure.

The main contributions of the paper are the following:

(i) The equilibrium structure of the delayed fractional financial model is derived explicitly, including the existence condition for the nontrivial equilibria.

(ii) The linearized fractional delay system and its characteristic equation are obtained. The sign error that can occur at the equilibrium E_0 is corrected, and an explicit stability condition for E_0 is stated in terms of the roots of a quadratic polynomial in λ^ρ.

(iii) A numerical criterion for delay-dependent stability crossings at the nontrivial equilibria is formulated by reducing the characteristic equation to a complex modulus and phase condition.

(iv) A predict-evaluate-correct-evaluate (PECE) predictor-corrector algorithm is presented for the Caputo fractional delay system, including the treatment of delayed values through history functions and interpolation.

(v) Numerical comparisons are organized to isolate the roles of ρ and τ, including memory-order sweeps, delay sweeps, delayed versus nondelayed simulations, and fractional versus integer-order comparisons.

(vi) A residual-based verification strategy is included. The residual is computed with an independent quintic Caputo reconstruction derived from local interpolation and exact kernel moments.

The scope of the paper is also stated explicitly. The numerical experiments reported here are intended to demonstrate stability tendencies, transient amplification, memory smoothing, and residual consistency. They are not presented as a complete proof of chaos or as a full bifurcation classification. Establishing chaotic regimes would require a systematic study based on Lyapunov exponents, long-time convergence of attractors, continuation of stability switches, and parameter-plane scans. These tasks are left as future work.

The remainder of the paper is organized as follows: Section 2 introduces the delayed Caputo fractional financial system and derives its equilibria. Section 3 develops the local stability analysis and corrects the characteristic equation at E_0. Section 4 presents the predictor-corrector method and the residual estimator. Section 5 reports the comparative numerical experiments. Section 6 discusses the interpretation, strengths, and limitations of the study. Section 7 gives the conclusions and future directions.

2. Mathematical model

2.1. Model formulation

Let $x(t)$, $y(t)$, and $z(t)$ denote, respectively, the interest rate, investment demand, and price index at time t. The proposed delayed fractional financial model is

$$
\begin{aligned}
{}_0^C D_t^\rho x(t) &= z(t) + \big(y(t) - a\big)x(t), && (2.1)\\
{}_0^C D_t^\rho y(t) &= 1 - by(t) - x^2(t-\tau), && (2.2)\\
{}_0^C D_t^\rho z(t) &= -x(t) - cz(t), && (2.3)
\end{aligned}
$$

where $0 < \rho < 1$, $\tau \geq 0$, and $a, b, c > 0$. The parameter a represents a market-friction or saving-related effect in the interest-rate equation, b measures the linear relaxation of the investment demand, and c measures the dissipation rate of the price index.

The nonlinear term $x^2(t-\tau)$ is the only delayed term in the model. This choice is made for modeling and mathematical reasons. Economically, the squared interest-rate contribution represents a nonlinear inhibitory effect of borrowing conditions on investment demand. Such an effect is not expected to be instantaneous: Firms and investors typically respond to previously observed credit conditions, not only to the current interest rate. Mathematically, inserting the delay only in this channel creates a transparent delayed variant of the classical model and allows the influence of a single delayed feedback mechanism to be isolated. The terms $-by(t)$ and $(y(t)-a)x(t)$ are left nondelayed because they represent instantaneous adjustment and current coupling in the simplified model.

2.2. Caputo derivative and history data

For $0 < \rho < 1$, the Caputo derivative of a sufficiently smooth function u is defined by

$$
{}_0^C D_t^\rho u(t) = \frac{1}{\Gamma(1-\rho)} \int_0^t (t-s)^{-\rho} u'(s)\, ds. \qquad (2.4)
$$

This definition shows that the current fractional rate depends on the whole previous evolution of the function. Since the model contains the delayed value $x(t-\tau)$, the initial data must be prescribed on the history interval $[-\tau, 0]$:

$$
x(t) = \phi_1(t), \qquad y(t) = \phi_2(t), \qquad z(t) = \phi_3(t), \qquad -\tau \leq t \leq 0. \qquad (2.5)
$$

The history functions encode the state of the financial variables before the initial observation time.

2.3. Equilibrium points

At an equilibrium $E^* = (x^*, y^*, z^*)$, the state is constant and therefore $x(t-\tau) = x^*$. Setting the right-hand sides of (2.1)–(2.3) equal to zero gives

$$0 = z^* + (y^* - a)x^*, \tag{2.6}$$
$$0 = 1 - by^* - (x^*)^2, \tag{2.7}$$
$$0 = -x^* - cz^*. \tag{2.8}$$

From (2.8),

$$z^* = -\frac{x^*}{c}, \tag{2.9}$$

and from (2.7),

$$y^* = \frac{1-(x^*)^2}{b}. \tag{2.10}$$

Substitution into (2.6) gives

$$x^*\left[-\frac{1}{c} + \frac{1-(x^*)^2}{b} - a\right] = 0. \tag{2.11}$$

Therefore, the model always has the equilibrium

$$E_0 = \left(0, \frac{1}{b}, 0\right). \tag{2.12}$$

If $x^* \neq 0$, then

$$(x^*)^2 = 1 - ab - \frac{b}{c}. \tag{2.13}$$

Let

$$\Delta = 1 - ab - \frac{b}{c}. \tag{2.14}$$

When $\Delta > 0$, two additional equilibria exist:

$$E_\pm = \left(\pm\sqrt{\Delta},\ a + \frac{1}{c},\ \mp\frac{1}{c}\sqrt{\Delta}\right). \tag{2.15}$$

Thus, the delay does not change the equilibrium coordinates, but it affects the stability of nontrivial equilibria through the perturbation equations.

Remark 1. *The model is a delayed variant of the classical financial system. Its novelty is not the creation of a completely new three-dimensional economic structure, but the combined treatment of Caputo memory, a selected delayed nonlinear investment feedback, explicit stability formulas, comparative parameter studies, and residual-verified computation.*

3. Local stability analysis

3.1. Linearization around an equilibrium

Let $E^* = (x^*, y^*, z^*)$ be any equilibrium and introduce perturbations

$$x(t) = x^* + u(t), \qquad y(t) = y^* + v(t), \qquad z(t) = z^* + w(t). \tag{3.1}$$

Neglecting higher-order nonlinear terms gives

$$ {}_0^C D_t^\rho u(t) = (y^* - a)u(t) + x^* v(t) + w(t), \tag{3.2}$$
$$ {}_0^C D_t^\rho v(t) = -bv(t) - 2x^* u(t-\tau), \tag{3.3}$$
$$ {}_0^C D_t^\rho w(t) = -u(t) - cw(t). \tag{3.4}$$

Equivalently,

$$ {}_0^C D_t^\rho U(t) = A_0 U(t) + A_1 U(t-\tau), \tag{3.5}$$

where $U = (u, v, w)^T$ and

$$A_0 = \begin{pmatrix} y^* - a & x^* & 1 \\ 0 & -b & 0 \\ -1 & 0 & -c \end{pmatrix}, \qquad A_1 = \begin{pmatrix} 0 & 0 & 0 \\ -2x^* & 0 & 0 \\ 0 & 0 & 0 \end{pmatrix}. \tag{3.6}$$

3.2. Characteristic equation

Using the exponential ansatz $U(t) = \eta e^{\lambda t}$, one obtains formally

$$\left(\lambda^\rho I - A_0 - A_1 e^{-\lambda\tau}\right)\eta = 0. \tag{3.7}$$

Therefore, the characteristic equation is

$$\det\left(\lambda^\rho I - A_0 - A_1 e^{-\lambda\tau}\right) = 0. \tag{3.8}$$

For the present model, this becomes

$$(\lambda^\rho - (y^* - a))(\lambda^\rho + b)(\lambda^\rho + c) + 2(x^*)^2(\lambda^\rho + c)e^{-\lambda\tau} + (\lambda^\rho + b) = 0. \tag{3.9}$$

This equation contains both the fractional spectral power λ^ρ and the delay factor $e^{-\lambda\tau}$. Consequently, the delay-dependent stability problem is transcendental.

3.3. Corrected characteristic equation at E_0

At

$$E_0 = \left(0, \frac{1}{b}, 0\right),$$

one has $x^* = 0$ and $y^* - a = 1/b - a$. Therefore, the delayed contribution disappears at the linear level, and the characteristic equation reduces to

$$\left(\lambda^\rho - \left(\frac{1}{b} - a\right)\right)(\lambda^\rho + b)(\lambda^\rho + c) + (\lambda^\rho + b) = 0. \tag{3.10}$$

Equivalently,

$$(\lambda^\rho + b)\left[\left(\lambda^\rho - \left(\frac{1}{b} - a\right)\right)(\lambda^\rho + c) + 1\right] = 0. \tag{3.11}$$

This is the corrected expression. In particular,

$$\lambda^\rho - \left(\frac{1}{b} - a\right) = \lambda^\rho - \frac{1}{b} + a, \tag{3.12}$$

not $\lambda^\rho - 1/b - a$.

Set $\mu = \lambda^\rho$ and

$$d = \frac{1}{b} - a. \tag{3.13}$$

Then (3.11) gives

$$\mu_1 = -b, \tag{3.14}$$

and

$$(\mu - d)(\mu + c) + 1 = 0. \tag{3.15}$$

That is,

$$\mu^2 + (c - d)\mu + (1 - cd) = 0. \tag{3.16}$$

Thus,

$$\mu_\pm = \frac{-(c-d) \pm \sqrt{(c-d)^2 - 4(1-cd)}}{2}, \qquad d = \frac{1}{b} - a. \tag{3.17}$$

In terms of a, b, c, this may be written as

$$\mu_\pm = \frac{-\left(a + c - \frac{1}{b}\right) \pm \sqrt{\left(a + c - \frac{1}{b}\right)^2 - 4\left(1 + ac - \frac{c}{b}\right)}}{2}. \tag{3.18}$$

Proposition 1 (Local stability of E_0)**.** *For the commensurate Caputo fractional system of order* $0 < \rho < 1$*, the equilibrium* E_0 *is locally asymptotically stable if the spectral values* $\mu_1 = -b$*,* μ_+*, and* μ_- *satisfy*

$$|\arg(\mu_k)| > \frac{\rho\pi}{2}, \qquad k = 1, +, -. \tag{3.19}$$

Equivalently,

$$\rho < \frac{2}{\pi} \min_{k \in \{1,+,-\}} |\arg(\mu_k)|. \tag{3.20}$$

Since $\mu_1 = -b < 0$*, this root always satisfies the fractional stability condition for* $0 < \rho < 1$*. Hence, the stability of* E_0 *is determined by* μ_+ *and* μ_-*.*

Proof. For a commensurate linear Caputo system ${}_0^C D_t^\rho U = AU$, Matignon's criterion requires every eigenvalue μ of A to satisfy $|\arg(\mu)| > \rho\pi/2$. At E_0, the delayed term vanishes in the linearization, and the spectrum is determined by (3.14) and (3.17). Applying the criterion gives (3.19) and (3.20). Since $-b$ lies on the negative real axis, $|\arg(-b)| = \pi$, and therefore $-b$ is admissible for all $0 < \rho < 1$. □

3.4. Characteristic equation at $E_\pm$

When $\Delta > 0$, the nontrivial equilibria are

$$E_\pm = \left(\pm\sqrt{\Delta},\ a + \frac{1}{c},\ \mp\frac{\sqrt{\Delta}}{c}\right), \qquad \Delta = 1 - ab - \frac{b}{c}.$$

For these equilibria,

$$y^* - a = \frac{1}{c}, \qquad (x^*)^2 = \Delta. \tag{3.21}$$

Therefore, (3.9) becomes

$$\left(\lambda^\rho - \frac{1}{c}\right)(\lambda^\rho + b)(\lambda^\rho + c) + 2\Delta(\lambda^\rho + c)e^{-\lambda\tau} + (\lambda^\rho + b) = 0. \tag{3.22}$$

Unlike E_0, the stability of $E_\pm$ depends directly on τ.

For numerical stability-boundary computations, write

$$\mu(\omega) = \lambda^\rho = (i\omega)^\rho = \omega^\rho\left[\cos\left(\frac{\rho\pi}{2}\right) + i\sin\left(\frac{\rho\pi}{2}\right)\right], \qquad \omega > 0. \tag{3.23}$$

Then (3.22) can be written as

$$A(\omega) + B(\omega)e^{-i\omega\tau} = 0, \tag{3.24}$$

where

$$A(\omega) = \left(\mu(\omega) - \frac{1}{c}\right)(\mu(\omega) + b)(\mu(\omega) + c) + \mu(\omega) + b, \tag{3.25}$$

$$B(\omega) = 2\Delta(\mu(\omega) + c). \tag{3.26}$$

Since $|e^{-i\omega\tau}| = 1$, a possible imaginary-axis crossing must satisfy

$$|A(\omega)| = |B(\omega)|. \tag{3.27}$$

For every positive solution ω_* of (3.27), candidate critical delays are obtained from the phase relation

$$\tau_k(\omega_*) = \frac{\arg(-A(\omega_*)/B(\omega_*)) + 2k\pi}{\omega_*}, \qquad k = 0, 1, 2, \ldots, \tag{3.28}$$

retaining only positive values of τ_k. Equations (3.27) and (3.28) provide a practical numerical criterion for locating delay-dependent stability boundaries.

3.5. Interpretation of the stability analysis

The stability analysis shows two distinct mechanisms. At E_0, the delay is absent from the linearized dynamics because the coefficient multiplying the delayed perturbation is proportional to x^*. Consequently, the stability of E_0 depends only on a, b, c, and ρ. At $E_\pm$, however, the delayed term enters the characteristic equation and may shift characteristic roots across the fractional stability boundary. Thus, the nontrivial equilibria are the natural locations where delay-induced stability switches may occur.

The fractional order modifies the angular stability sector. Smaller values of ρ reduce the unstable sector and may stabilize spectral configurations that are unstable in the integer-order case. In economic terms, this reflects a smoothing effect of memory: Accumulated past behavior can moderate the immediate effect of delayed feedback. The delay parameter, by contrast, can amplify oscillatory tendencies because the current investment response is based on past interest-rate information.

4. Numerical method and residual verification

4.1. Volterra integral formulation

Let

$$X(t) = \begin{pmatrix} x(t) \\ y(t) \\ z(t) \end{pmatrix}, \qquad F(t, X(t), X(t-\tau)) = \begin{pmatrix} z(t) + (y(t) - a)x(t) \\ 1 - by(t) - x^2(t-\tau) \\ -x(t) - cz(t) \end{pmatrix}. \tag{4.1}$$

Then the system can be written as

$${}_0^C D_t^\rho X(t) = F(t, X(t), X(t-\tau)). \tag{4.2}$$

For $0 < \rho < 1$, this is equivalent to the Volterra integral equation

$$X(t) = X(0) + \frac{1}{\Gamma(\rho)} \int_0^t (t-s)^{\rho-1} F(s, X(s), X(s-\tau))\, ds. \tag{4.3}$$

This integral form is the basis of the numerical method.

4.2. PECE predictor-corrector scheme

Let $t_n = nh$, $n = 0, 1, \ldots, N$, with $Nh = T$, and write $X_n \approx X(t_n)$. Define

$$F_j = F(t_j, X_j, X_j^\tau), \tag{4.4}$$

where $X_j^\tau \approx X(t_j - \tau)$. The predictor is

$$X_{n+1}^P = X_0 + \frac{h^\rho}{\Gamma(\rho+1)} \sum_{j=0}^{n} b_{j,n+1} F_j, \tag{4.5}$$

where

$$b_{j,n+1} = (n+1-j)^\rho - (n-j)^\rho. \tag{4.6}$$

The corrector is

$$X_{n+1} = X_0 + \frac{h^\rho}{\Gamma(\rho+2)} \left[F(t_{n+1}, X_{n+1}^P, (X_{n+1}^P)^\tau) + \sum_{j=0}^{n} a_{j,n+1} F_j \right], \tag{4.7}$$

where

$$a_{0,n+1} = n^{\rho+1} - (n-\rho)(n+1)^\rho, \tag{4.8}$$

$$a_{j,n+1} = (n-j+2)^{\rho+1} - 2(n-j+1)^{\rho+1} + (n-j)^{\rho+1}, \quad 1 \le j \le n, \tag{4.9}$$

$$a_{n+1,n+1} = 1. \tag{4.10}$$

This is the fractional Adams-Bashforth-Moulton PECE scheme commonly used for Caputo systems and adaptable to delay equations [16–18].

4.3. Evaluation of the delayed value

If $t_j - \tau < 0$, the delayed state is obtained from the history function:

$$X_j^{\tau} = \Phi(t_j - \tau), \qquad \Phi = (\phi_1, \phi_2, \phi_3)^T. \tag{4.11}$$

If $t_j - \tau \geq 0$ and $\tau = mh$ for an integer m, then

$$X_j^{\tau} = X_{j-m}. \tag{4.12}$$

If $\tau/h \notin \mathbb{N}$, linear interpolation is used. If $t_j - \tau \in [t_k, t_{k+1}]$, then

$$X(t_j - \tau) \approx X_k + \frac{t_j - \tau - t_k}{h}(X_{k+1} - X_k). \tag{4.13}$$

Higher-order interpolation can be used, but linear interpolation is sufficient for the comparative experiments reported here.

4.4. Quintic Caputo residual: Derivation

Because no closed-form exact solution is available, the numerical solution is checked by a defect residual. The key point is that the residual derivative is not recomputed with the same PECE formula. Instead, it is reconstructed through an independent local quintic approximation of the Caputo derivative.

For a mesh point $t_k = kh$, the Caputo derivative is decomposed over cells:

$${}_0^C D_t^{\rho} f(t_k) = \frac{1}{\Gamma(1-\rho)} \sum_{j=1}^{k} \int_{t_{j-1}}^{t_j} (t_k - s)^{-\rho} f'(s)\, ds. \tag{4.14}$$

On the cell $[t_{j-1}, t_j]$, set $s = t_{j-1} + h\theta$, $0 \leq \theta \leq 1$, and $m = k - j$. Then

$$t_k - s = h(m + 1 - \theta). \tag{4.15}$$

Let $p_j(\theta)$ be the quintic interpolant of f on the six local nodes

$$\theta_0 = 0, \tag{4.16}$$

$$\theta_1 = \frac{3}{8} - \frac{\sqrt{5}}{8}, \tag{4.17}$$

$$\theta_2 = \frac{5}{8} - \frac{\sqrt{5}}{8}, \tag{4.18}$$

$$\theta_3 = \frac{3}{8} + \frac{\sqrt{5}}{8}, \tag{4.19}$$

$$\theta_4 = \frac{5}{8} + \frac{\sqrt{5}}{8}, \tag{4.20}$$

$$\theta_5 = 1. \tag{4.21}$$

Thus,

$$p_j(\theta) = \sum_{r=0}^{5} f(t_{j,r}^{(5)})L_r(\theta), \qquad t_{j,r}^{(5)} = t_{j-1} + h\theta_r, \tag{4.22}$$

where L_r are the Lagrange basis polynomials. Since $f'(s) \approx h^{-1}p_j'(\theta)$, one obtains

$${}_0^C D_t^\rho f(t_k) \approx \frac{h^{-\rho}}{\Gamma(1-\rho)} \sum_{j=1}^{k} \sum_{r=0}^{5} \omega_{r,k-j}^{(5)}(\rho) f(t_{j,r}^{(5)}), \tag{4.23}$$

where

$$\omega_{r,m}^{(5)}(\rho) = \int_0^1 (m+1-\theta)^{-\rho} L_r'(\theta)\, d\theta. \tag{4.24}$$

Because $L_r'(\theta)$ is a polynomial of degree four, each weight can be expressed as a linear combination of the moments

$$M_q(m,\rho) = \int_0^1 \theta^q (m+1-\theta)^{-\rho}\, d\theta, \qquad q = 0,1,2,3,4. \tag{4.25}$$

The explicit closed forms of these moments are

$$M_0(m,\rho) = \frac{(m+1)^{1-\rho} - m^{1-\rho}}{1-\rho}, \tag{4.26}$$

$$M_1(m,\rho) = (m+1)M_0(m,\rho) - \frac{(m+1)^{2-\rho} - m^{2-\rho}}{2-\rho}, \tag{4.27}$$

$$M_2(m,\rho) = (m+1)^2 M_0(m,\rho) - \frac{2(m+1)[(m+1)^{2-\rho} - m^{2-\rho}]}{2-\rho} + \frac{(m+1)^{3-\rho} - m^{3-\rho}}{3-\rho}, \tag{4.28}$$

$$\begin{aligned} M_3(m,\rho) = &(m+1)^3 M_0(m,\rho) - \frac{3(m+1)^2[(m+1)^{2-\rho} - m^{2-\rho}]}{2-\rho} + \frac{3(m+1)[(m+1)^{3-\rho} - m^{3-\rho}]}{3-\rho} \\ &- \frac{(m+1)^{4-\rho} - m^{4-\rho}}{4-\rho}, \end{aligned} \tag{4.29}$$

$$\begin{aligned} M_4(m,\rho) = &(m+1)^4 M_0(m,\rho) - \frac{4(m+1)^3[(m+1)^{2-\rho} - m^{2-\rho}]}{2-\rho} + \frac{6(m+1)^2[(m+1)^{3-\rho} - m^{3-\rho}]}{3-\rho} \\ &- \frac{4(m+1)[(m+1)^{4-\rho} - m^{4-\rho}]}{4-\rho} + \frac{(m+1)^{5-\rho} - m^{5-\rho}}{5-\rho}. \end{aligned} \tag{4.30}$$

The weights used in the computation are obtained by expanding $L_r'(\theta)$ and inserting the coefficients into (4.25). Therefore, the quintic residual operator follows directly from polynomial interpolation and exact integration of the weakly singular Caputo kernel.

4.5. Residual definitions

Let (x_h, y_h, z_h) be the PECE solution. The residuals are defined by

$$R_1(t_k) = Q_h^\rho[x_h](t_k) - \left[z_h(t_k) + (y_h(t_k) - a)x_h(t_k)\right], \tag{4.31}$$

$$R_2(t_k) = Q_h^\rho[y_h](t_k) - \left[1 - by_h(t_k) - x_h^2(t_k - \tau)\right], \tag{4.32}$$

$$R_3(t_k) = Q_h^\rho[z_h](t_k) - \left[-x_h(t_k) - cz_h(t_k)\right], \tag{4.33}$$

where Q_h^ρ denotes the quintic Caputo reconstruction in (4.23). A scalar residual measure is

$$R_{\text{glob}}(t_k) = \sqrt{R_1(t_k)^2 + R_2(t_k)^2 + R_3(t_k)^2}. \tag{4.34}$$

The residual is not the exact solution error. It is a defect indicator measuring how well the computed trajectory satisfies the original equations when the fractional derivative is independently reconstructed. Large residuals indicate time regions where the numerical trajectory is less reliable or where the mesh should be refined.

5. Numerical results

5.1. Example 1: Baseline transient response

We first consider a baseline computation in order to illustrate the finite-time response of the delayed Caputo financial system and to provide a reference case for the subsequent parameter comparisons. The fractional order and model parameters are chosen as

$$\rho = 0.98, \qquad a = 0.80, \qquad b = 0.20, \qquad c = 1.00, \qquad \tau = 0.80. \tag{5.1}$$

The constant history functions are prescribed by

$$x(t) = 0.20, \qquad y(t) = 1.10, \qquad z(t) = 0.10, \qquad -\tau \le t \le 0. \tag{5.2}$$

The integration interval is $0 \le t \le 10$, and the step size used in the baseline run is $h = 0.01$.

For these parameters,

$$\Delta = 1 - ab - \frac{b}{c} = 1 - (0.80)(0.20) - 0.20 = 0.64 > 0. \tag{5.3}$$

Therefore, the system possesses the three equilibria

$$E_0 = (0, 5, 0), \qquad E_+ = (0.8, 1.8, -0.8), \qquad E_- = (-0.8, 1.8, 0.8). \tag{5.4}$$

These equilibria are independent of the delay parameter τ, since the delayed variable coincides with the present variable at a constant state. Consequently, the role of τ is not to change the equilibrium coordinates but to modify the transient dynamics and the stability properties of perturbations around the equilibria.

A numerical summary of the baseline computation is reported in Table 1. The solution remains bounded on the interval $0 \le t \le 10$. The largest excursion occurs in the investment-demand component $y(t)$, whose maximum absolute value is approximately 8.016. The interest-rate and price-index components remain smaller in magnitude, with $\max|x(t)| \approx 0.6393$ and $\max|z(t)| \approx 0.4298$. At the final time, all three variables have decreased substantially in magnitude, which indicates that the large response observed in this experiment is a finite-time transient rather than evidence of a sustained attractor.

Table 1. Numerical summary of the baseline computation for $\rho = 0.98$, $a = 0.80$, $b = 0.20$, $c = 1.00$, $\tau = 0.80$, $T = 10$, and $h = 0.01$.

Quantity	**Value**
$\max \lvert x(t) \rvert$	0.6393
$\max \lvert y(t) \rvert$	8.016
$\max \lvert z(t) \rvert$	0.4298
$x(T)$	-4.5462×10^{-3}
$y(T)$	1.6046×10^{-1}
$z(T)$	-3.6865×10^{-3}
$\Delta = 1 - ab - b/c$	6.4×10^{-1}
E_0	$(0, 5, 0)$
E_+	$(0.8, 1.8, -0.8)$
E_-	$(-0.8, 1.8, 0.8)$

The time series in Figure 1 show a pronounced finite-time transient. The investment demand $y(t)$ exhibits the dominant excursion, while $x(t)$ and $z(t)$ follow the transient at smaller amplitudes. The corresponding absolute values in Figure 2 identify the time window in which the nonlinear delayed feedback is strongest.

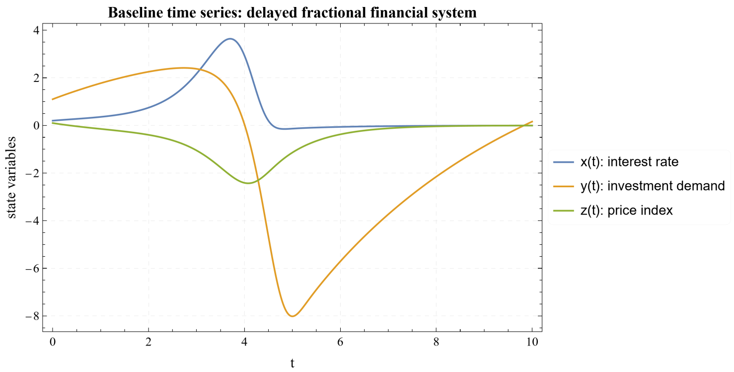

Figure 1. Baseline time series of $x(t)$, $y(t)$, and $z(t)$ for $\rho = 0.98$, $a = 0.80$, $b = 0.20$, $c = 1.00$, and $\tau = 0.80$. The delayed nonlinear investment feedback produces a large but finite transient, especially in the investment-demand component.

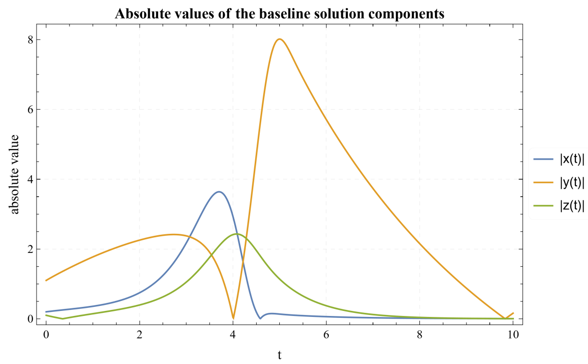

Figure 2. Absolute values of the baseline state variables. The dominant activity is localized in the transient interval, which is also the region where the residual diagnostic reaches its largest values.

The phase projections in Figures 3 and 4 should be interpreted as finite-time transient trajectories. They show the geometry of the computed orbit on the finite interval $0 \leq t \leq 10$, but they are not claimed to represent a periodic orbit or a chaotic attractor. This distinction is important because a finite phase curve alone is not sufficient evidence for asymptotic periodicity or chaos.

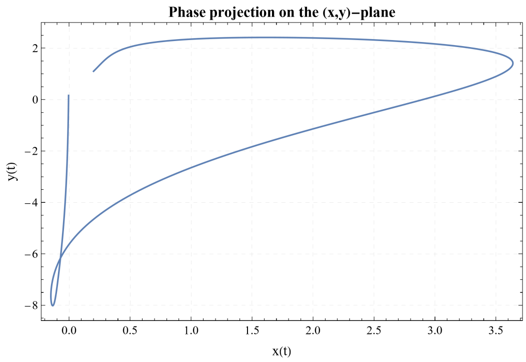

(a) Projection on the (x, y)-plane.

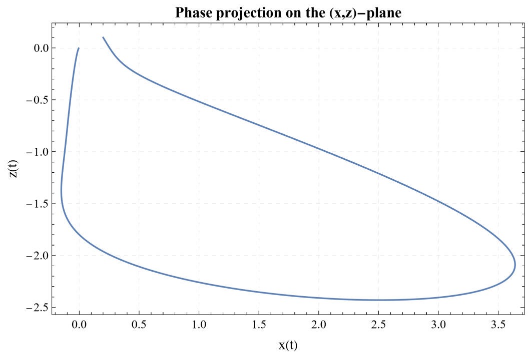

(b) Projection on the (x, z)-plane.

Figure 3. Two-dimensional phase projections of the baseline finite-time trajectory. The curves show transient geometry generated by the interaction between fractional memory and delayed investment feedback.

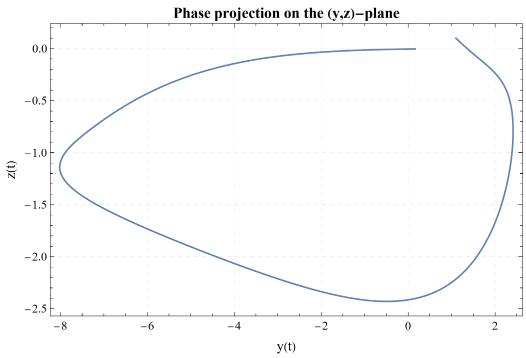

(a) Projection on the (y, z)-plane.

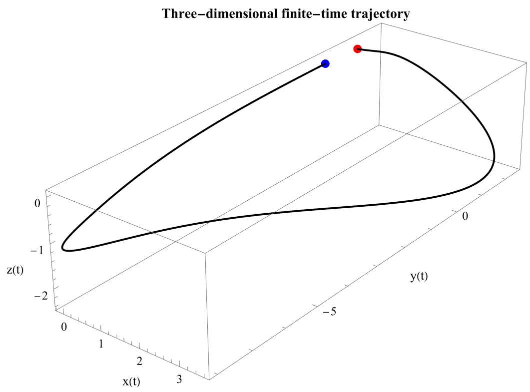

(b) Three-dimensional trajectory.

Figure 4. Additional phase views of the baseline computation. The figures show a bounded transient path and illustrate the non-monotone coupling among the interest rate, investment demand, and price index.

Overall, the baseline computation shows that the delayed nonlinear investment term can generate a strong transient amplification of the investment-demand variable. However, the numerical evidence in this example supports only a bounded finite-time transient response. It is therefore described as a transient trajectory rather than as a periodic orbit, bifurcation branch, or chaotic attractor.

5.2. Example 2: Influence of memory order and delay

The second numerical experiment is designed to answer two questions raised by the reviewers: How the fractional order modifies the transient response, and how the explicit investment delay changes the dynamics when all other parameters are fixed. The baseline parameters used in these comparisons are summarized in Table 2. For this set,

$$\Delta = 1 - ab - \frac{b}{c} = 1 - (0.80)(0.20) - 0.20 = 0.64 > 0,$$

and therefore the three equilibria exist:

$$E_0 = (0, 5, 0), \qquad E_+ = (0.8, 1.8, -0.8), \qquad E_- = (-0.8, 1.8, 0.8).$$

The coordinates of these equilibria do not depend on the delay parameter τ. Consequently, any change observed when τ is varied is caused by the delayed perturbation dynamics rather than by a displacement of the stationary states.

Table 2. Parameter values used in the second numerical experiment. The same history functions $x(t) = 0.20$, $y(t) = 1.10$, and $z(t) = 0.10$ are imposed for $-\tau \leq t \leq 0$.

Quantity	**Value**
Market parameter a	0.80
Investment damping b	0.20
Price-index damping c	1.00
Baseline fractional order ρ	0.98
Baseline delay τ	0.80
Final time T	10
Step size h	0.01
Equilibrium discriminant $\Delta = 1 - ab - b/c$	0.64
Trivial equilibrium E_0	$(0, 5, 0)$
Positive equilibrium E_+	$(0.8, 1.8, -0.8)$
Negative equilibrium E_-	$(-0.8, 1.8, 0.8)$
Fractional-order sweep	$\rho \in \{0.70, 0.80, 0.90, 0.98\}$
Delay sweep	$\tau \in \{0, 0.40, 0.80, 1.20\}$

5.2.1. Effect of the fractional order

To isolate the role of memory, the fractional order is varied according to

$$\rho \in \{0.70, 0.80, 0.90, 0.98\},$$

while $a = 0.80$, $b = 0.20$, $c = 1.00$, $\tau = 0.80$, and the history functions are kept fixed. This experiment is not intended to establish a full bifurcation scenario. Its purpose is more focused: to show that the fractional order is an active dynamical parameter that changes the amplitude, timing, and duration of the transient investment response.

The curves in Figure 5 show that changing ρ affects the transient regime without changing the equilibrium coordinates. Smaller values of ρ correspond to stronger memory effects and tend to smooth the response, whereas values closer to the integer-order limit allow sharper transient variations. This supports the interpretation that fractional memory can moderate the destabilizing influence of delayed nonlinear investment feedback.

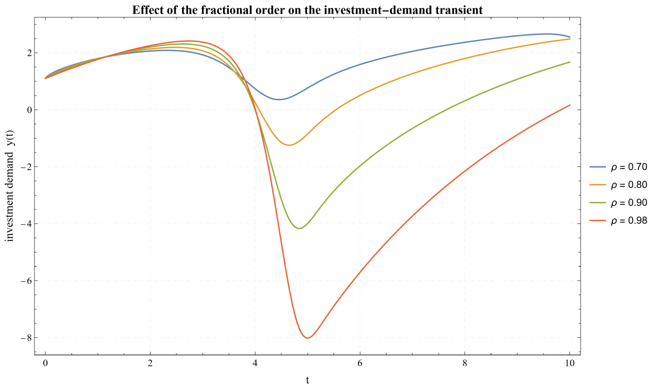

Figure 5. Investment-demand response $y(t)$ for $\rho = 0.70, 0.80, 0.90, 0.98$, with $a = 0.80$, $b = 0.20$, $c = 1.00$, and $\tau = 0.80$. The comparison shows that the memory order modifies both the size and the persistence of the transient excursion.

5.2.2. Effect of the delay

To isolate the effect of delayed investment response, the delay is varied as

$$\tau \in \{0, 0.40, 0.80, 1.20\},$$

while $\rho = 0.98$, $a = 0.80$, $b = 0.20$, $c = 1.00$, and the same initial history are used. This comparison includes the nondelayed case $\tau = 0$ and three delayed cases.

Figure 6 confirms that the delay parameter has a direct influence on the transient dynamics. Since the equilibria are independent of τ, the observed differences are not caused by a change of stationary state. Instead, they arise from the delayed nonlinear feedback term $x^2(t - \tau)$, which modifies the way perturbations are transferred into the investment equation. In this sense, the delay acts as a genuine dynamical mechanism.

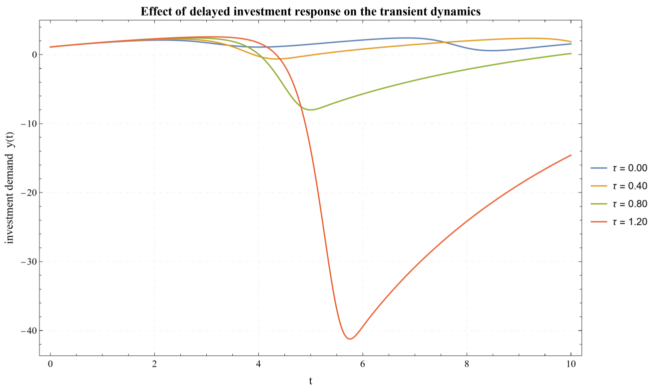

Figure 6. Investment-demand response $y(t)$ for $\tau = 0, 0.40, 0.80, 1.20$, with $\rho = 0.98$ and the remaining parameters fixed. The figure shows that the delay changes the amplitude and timing of the transient response, even though the equilibria are unchanged.

5.2.3. Delayed versus nondelayed dynamics

A direct comparison between the nondelayed model and the delayed model is presented in Figure 7. Both computations use the same values of a, b, c, ρ, the same history functions, and the same numerical step size. The only change is the replacement of $\tau = 0$ by $\tau = 0.80$.

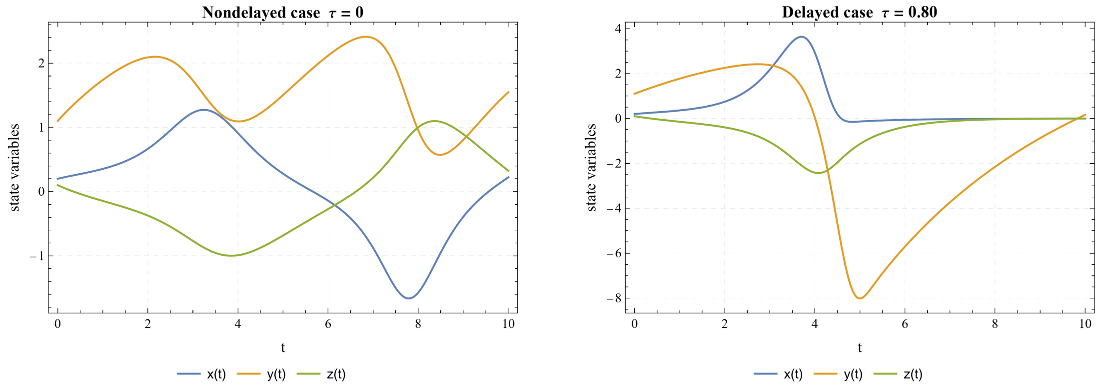

Figure 7. Side-by-side comparison between the nondelayed case $\tau = 0$ and the delayed case $\tau = 0.80$, with $\rho = 0.98$. The delayed feedback shifts and amplifies the transient response, showing explicitly what the investment lag contributes to the dynamics.

This comparison answers the modeling question of why the delay is included. The lagged term does not create new equilibria, but it changes the finite-time trajectory followed by the system before relaxation. Therefore, the delay should be interpreted as a mechanism that modifies the adjustment process rather than as a parameter that changes the algebraic equilibrium structure.

5.2.4. Fractional versus integer-order response

Finally, to separate fractional memory from the classical integer-order limit, Figure 8 compares the fractional case $\rho = 0.98$ with the integer-order case $\rho = 1$. The fractional curve is computed with the PECE scheme, whereas the integer-order delayed system is computed with a delayed ordinary differential equation solver. In both cases, the parameters $a = 0.80$, $b = 0.20$, $c = 1.00$, $\tau = 0.80$, and the same initial history are used.

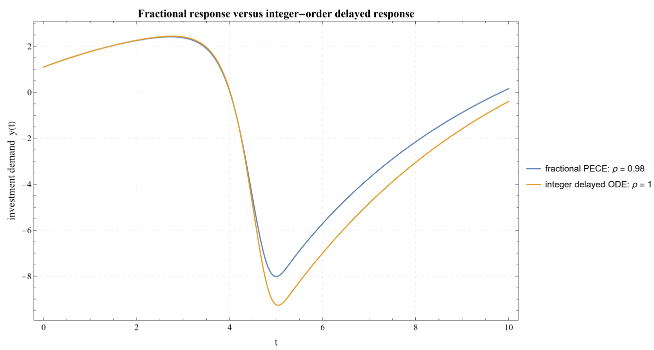

Figure 8. Comparison between the fractional response $\rho = 0.98$ and the integer-order delayed response $\rho = 1$. Even when the fractional order is close to one, the memory term changes the amplitude, phase, and relaxation of the investment-demand transient.

The comparison shows that the fractional model is not merely a cosmetic modification of the integer-order delayed system. Even for $\rho = 0.98$, the memory effect changes the transient response. This reinforces the main conclusion of the numerical study: Delayed investment feedback and fractional memory act together, but they influence the dynamics in different ways. The delay changes the timing and amplification of the response, while the fractional order controls the strength of memory-induced smoothing.

5.3. Residual diagnostics and mesh refinement

The residual curves for the baseline computation are displayed in Figure 9. The residual was evaluated over the full time mesh, not only at a few selected sample points. This point is important because the largest residual values occur in a short transient interval, precisely when the investment-demand variable $y(t)$ undergoes its strongest excursion. This behavior is expected, since the delayed quadratic feedback term $x^2(t-\tau)$ appears directly in the investment equation and becomes most active during the rapid transient response.

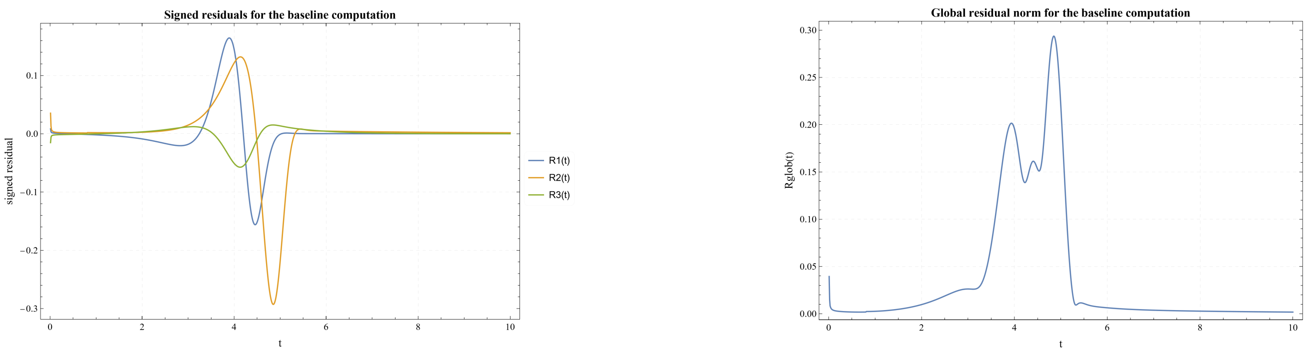

(a) Signed residuals. **(b)** Global residual norm.

Figure 9. Residual diagnostics for the baseline computation with $\rho = 0.98$, $a = 0.80$, $b = 0.20$, $c = 1.00$, $\tau = 0.80$, and $h = 0.01$. The residual reaches its maximum during the strongest transient activity and decreases after the solution enters a smoother regime.

To verify that the residual behavior is not an artifact of the chosen time step, a mesh-refinement test was performed for h, $h/2$, and $h/4$, namely $h = 0.01$, 0.005, and 0.0025. For each run, the maximum residual was computed over the full mesh according to

$$R_{\max}(h) = \max_{1 \le k \le N} R_{\text{glob}}(t_k), \tag{5.5}$$

and the empirical decay rate was estimated by

$$p_h = \frac{\log(R_{\max}(h)/R_{\max}(h/2))}{\log 2}. \tag{5.6}$$

The residual decrease under mesh refinement is illustrated in Figure 10.

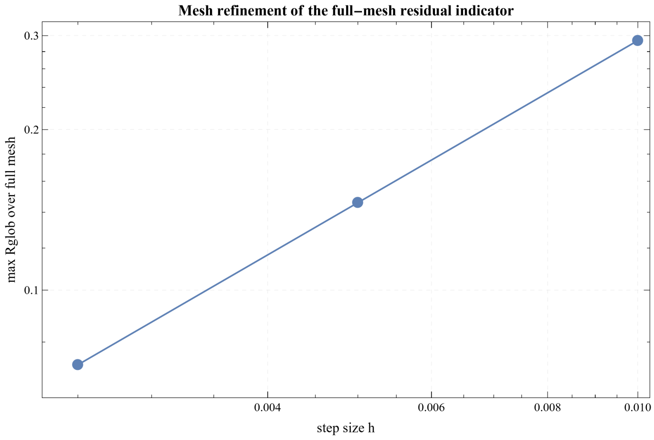

Figure 10. Mesh refinement test for the full-mesh residual indicator using $h = 0.01$, $h/2 = 0.005$, and $h/4 = 0.0025$. The approximately monotone halving of $R_{\max}(h)$ under mesh refinement confirms that the residual defect is reduced as the temporal resolution is increased.

The refinement results in Table 3 show a clear decrease of the full-mesh residual maxima as the step size is reduced. In particular,

$$R_{\max}(0.01) = 0.293692, \qquad R_{\max}(0.005) = 0.145898, \qquad R_{\max}(0.0025) = 0.0724843.$$

Thus, halving the step size approximately halves the global residual defect, with empirical rates $p_h \approx 1.00934$ and $p_h \approx 1.00922$. The second residual component R_2 is the dominant one in all three computations, which is consistent with the fact that the delayed nonlinear term appears in the investment-demand equation. The time at which R_{glob} reaches its maximum is concentrated near $t \approx 4.85$, matching the transient interval observed in the solution profiles. This confirms that the largest numerical defect occurs where the delayed nonlinear feedback is strongest.

Table 3. Residual summary over the full mesh for the baseline computation. The maximum residual is not computed from sparse samples but from all available mesh points.

h	N	$\max\lvert R_1\rvert$	$\max\lvert R_2\rvert$	$\max\lvert R_3\rvert$	$\max R_{\text{glob}}$	p_h
0.0100	1000	0.16445	0.292792	0.0573452	0.293692	1.00934
0.0050	2000	0.0816702	0.14545	0.0284644	0.145898	1.00922
0.0025	4000	0.0405677	0.072258	0.0141363	0.0724843	–

These results address the numerical reliability issue directly: The residual peak is not missed by sparse sampling, and the defect decreases systematically under refinement. Therefore, the baseline step size $h = 0.01$ captures the qualitative transient structure, while the refined computations confirm the expected reduction of the residual indicator.

5.4. Numerical stability map

For the nontrivial equilibria $E_{\pm}$, the delay enters the characteristic equation explicitly. Therefore, although the equilibrium coordinates are independent of τ, their local stability may change when the delay is varied. To complement the analytical stability formulas, the delay-dependent characteristic equation was evaluated numerically, and the first critical crossing was located in the (ρ, τ)-plane.

The stability scan in Figure 11 should be interpreted as a local linear stability diagnostic, not as a full nonlinear bifurcation diagram. Its role is to provide concrete numerical information about the interaction between fractional memory and delayed investment response. In particular, it indicates how the stability boundary changes when the memory order ρ varies and confirms that the delay parameter acts through the perturbation dynamics rather than through the equilibrium coordinates themselves.

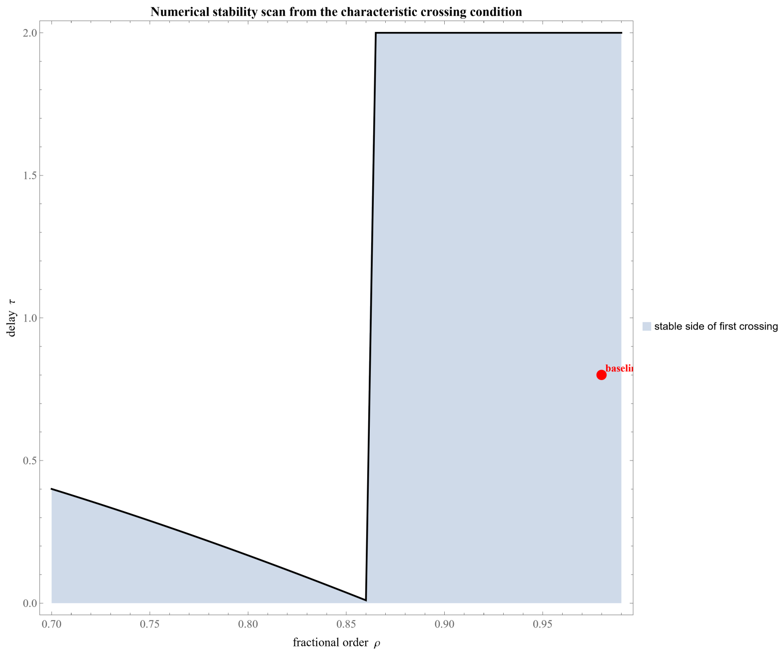

Figure 11. Numerical stability scan in the (ρ, τ)-plane for the nontrivial equilibria $E_{\pm}$. The curve represents the first characteristic crossing detected from the delay-dependent characteristic equation. The scan shows how the admissible delay before instability depends on the fractional order ρ.

6. Analysis and discussion

The numerical and analytical results obtained in the previous sections provide a coherent picture of the delayed Caputo financial system. The model contains two distinct mechanisms: distributed memory, introduced through the Caputo derivative of order $0 < \rho < 1$, and a discrete investment-response lag, introduced through the delayed nonlinear feedback term $x^2(t-\tau)$. The main conclusion is that these two mechanisms do not act in the same way. Fractional memory changes the rate, amplitude, and smoothing of the transient response, whereas the delay changes the timing and amplification of the investment feedback.

The results should be interpreted within the revised scope of the paper. The simulations demonstrate bounded finite-time transient dynamics, memory-induced smoothing, delay-induced amplification, and numerical consistency under residual refinement. They are not presented as a complete bifurcation analysis or as proof of a chaotic attractor. This distinction is essential because finite-time phase portraits alone cannot establish periodicity or chaos. A full chaos classification would require additional diagnostics, such as long-time Lyapunov exponents, continuation of stability switches, recurrence analysis, and systematic two-parameter exploration.

6.1. Interaction between fractional memory and delayed investment response

The fractional order ρ modifies the memory kernel in the Caputo derivative. When ρ is closer to one, the system behaves more similarly to the classical integer-order model and can exhibit sharper transient variations. When ρ is decreased, the memory effect becomes stronger, and the response tends to be smoother. This tendency agrees with the general role of fractional derivatives in dynamical systems: The present evolution is not determined only by the instantaneous state but by a weighted accumulation of past states [12–14].

The delay parameter τ, by contrast, introduces a discrete response lag into the investment equation. The term $x^2(t - \tau)$ represents the inhibitory effect of previously observed interest-rate conditions on current investment demand. Therefore, increasing τ does not change the algebraic equilibria, but it can change the path followed by the solution before it relaxes. This is consistent with the local stability analysis, where the delay appears through the factor $e^{-\lambda\tau}$ in the characteristic equation at the nontrivial equilibria $E_\pm$.

The parameter sweeps confirm this interpretation. Varying ρ while keeping τ fixed changes the amplitude and persistence of the transient investment response. Varying τ while keeping ρ fixed shifts and amplifies the transient response. Thus, the fractional order and the delay should be viewed as independent dynamical controls: One regulates memory smoothing, while the other regulates lagged feedback.

6.2. Stability interpretation

The local stability analysis reveals two different equilibrium scenarios. At

$$E_0 = \left(0, \frac{1}{b}, 0\right),$$

the delayed contribution disappears from the linearization because the coefficient multiplying the delayed perturbation is proportional to x^*. Consequently, the delay parameter τ does not influence the local stability of E_0 at the linear level. The stability of this equilibrium is controlled by the roots $\mu_1 = -b$ and $\mu_\pm$ obtained from the corrected quadratic equation in $\mu = \lambda^\rho$. The fractional stability criterion

$$|\arg(\mu_k)| > \frac{\rho\pi}{2},$$

then determines the admissible range of ρ.

The nontrivial equilibria $E_\pm$ behave differently. Since

$$(x^*)^2 = \Delta = 1 - ab - \frac{b}{c} > 0,$$

at these equilibria, the delayed feedback appears explicitly in the characteristic equation. The corresponding characteristic equation is transcendental, and a closed-form classification of all roots is generally not available. The numerical crossing criterion based on

$$|A(\omega)| = |B(\omega)|,$$

and the associated phase condition provides a practical way to detect the first delay-induced stability boundary.

The stability scan in the (ρ, τ)-plane should therefore be understood as a local linear diagnostic. It is not a nonlinear bifurcation diagram. Nevertheless, it is useful because it connects the analytical characteristic equation with the numerical simulations. In particular, it confirms that the delay affects the perturbation dynamics around $E_{\pm}$, while the equilibrium coordinates themselves remain unchanged.

6.3. Interpretation of the baseline dynamics

For the baseline parameter set

$$\rho = 0.98, \qquad a = 0.80, \qquad b = 0.20, \qquad c = 1.00, \qquad \tau = 0.80,$$

the discriminant is

$$\Delta = 1 - ab - \frac{b}{c} = 0.64 > 0.$$

Thus, the three equilibria E_0, E_+, and E_- exist. The computed trajectory remains bounded on the interval $0 \leq t \leq 10$, and the largest excursion occurs in the investment-demand variable $y(t)$. This is expected because the delay is inserted directly into the investment equation.

The numerical values reported in Table 1 show that

$$\max|y(t)| \approx 8.016, \qquad \max|x(t)| \approx 0.6393, \qquad \max|z(t)| \approx 0.4298.$$

Thus, the investment-demand component is the dominant transient variable in this experiment. At the final time, the values of $x(T)$, $y(T)$, and $z(T)$ are much smaller in magnitude than the transient peak, which supports the interpretation of the computed response as a finite-time transient rather than a sustained oscillatory or chaotic regime.

The phase projections should be interpreted with the same caution. They show a bounded nonlinear path in the projected phase planes and in three dimensions, but they do not establish the existence of an attractor. A finite-time trajectory may look loop-like without being periodic, and it may look geometrically complex without being chaotic. For this reason, the revised manuscript describes these curves as finite-time transient trajectories.

6.4. Comparison with nondelayed and integer-order cases

The delayed versus nondelayed comparison isolates the effect of τ. Since the same initial history and parameters are used in both runs, the differences between the curves are caused by the lagged nonlinear feedback. The delayed case shows that investment response can be shifted and amplified even though the equilibrium coordinates remain fixed. This supports the modeling choice of placing the delay in the nonlinear investment-feedback term.

The fractional versus integer-order comparison isolates the effect of memory. Even for $\rho = 0.98$, which is close to the integer-order limit, the fractional response differs from the classical delayed response. This indicates that the fractional formulation is not merely a cosmetic modification of the integer-order model. The memory term can alter transient amplitude, phase, and relaxation rate. This observation is consistent with previous studies of fractional-order financial systems and delayed fractional dynamics [5, 8, 10].

Together, these comparisons clarify the separate roles of the two modeling ingredients. The delay controls when past interest-rate information enters the investment equation, while the fractional order controls how strongly the full history of the state influences the present response.

6.5. Residual diagnostics and numerical reliability

The residual analysis is a central part of the revised numerical validation. Since no exact solution is available for the nonlinear fractional delay system, the residual is used as a defect indicator. It measures how well the computed trajectory satisfies the original equations when the Caputo derivative is reconstructed independently by the quintic residual operator.

The largest residual values occur near the time interval where the investment variable experiences its strongest transient excursion. This is consistent with the structure of the model: The second equation contains the delayed quadratic term $x^2(t-\tau)$, and the numerical defect is largest when this nonlinear feedback is most active. In all refinement runs, the second residual component R_2 is dominant, which agrees with the fact that the delayed nonlinear term appears in the investment equation.

The mesh-refinement results provide additional reliability. The full-mesh maximum residual satisfies

$$R_{\max}(0.01) = 0.293692, \qquad R_{\max}(0.005) = 0.145898, \qquad R_{\max}(0.0025) = 0.0724843.$$

Thus, halving the step size approximately halves the maximum residual defect, with empirical rates close to one. This confirms that the residual peak is not a sparse-sampling artifact and that the numerical defect decreases systematically under refinement.

It is important, however, to distinguish residual defect from exact error. The residual does not give the exact distance between the numerical and exact solutions. Instead, it provides an internal consistency check. A small residual suggests that the computed trajectory satisfies the governing equations well under an independent Caputo reconstruction, while a large residual indicates a time interval where refinement or additional numerical care is needed.

6.6. Relation with previous work

The present study is connected to three lines of previous research. First, it extends the Ma–Chen class of nonlinear financial models by combining a Caputo fractional derivative with a selected delayed nonlinear investment feedback [1, 5, 6]. Second, it is related to studies of fractional financial systems with time delay, where memory and lag have been shown to influence complexity, stability, and transient behavior [8, 10]. Third, it is connected to the broader literature on fractional-order nonlinear systems, multistability, and social or economic complexity [3, 4, 11].

The contribution of the present paper is not to claim a new chaotic financial model. Rather, it provides a careful residual-verified analysis of a focused delayed fractional variant. The emphasis is on explicit equilibria, corrected linear stability at E_0, delay-dependent stability diagnostics at $E_{\pm}$, controlled parameter comparisons, and full-mesh residual verification.

6.7. Strengths of the study

The main strengths of the study are the following.

First, the model is simple enough to allow analytical calculations. The equilibria can be obtained explicitly, and the characteristic equation can be derived in closed form. This makes the stability discussion transparent.

Second, the role of the delay is clearly localized. Since the delay is inserted only in the nonlinear investment-feedback term, the numerical experiments can isolate the dynamical effect of delayed investment response.

Third, the paper separates the effects of memory and delay through dedicated comparisons. The ρ-sweep, the τ-sweep, the delayed versus nondelayed simulation, and the fractional versus integer-order comparison give a clearer interpretation than a single numerical trajectory would provide.

Fourth, the residual verification improves numerical credibility. The residual is computed independently from the PECE scheme, and the maximum residual is reported over the full mesh. This directly addresses the need for more reliable numerical evidence in fractional delay simulations.

Fifth, the claims are stated conservatively. The paper does not infer chaos from finite-time phase portraits, and it does not present a stability scan as a full nonlinear bifurcation diagram.

6.8. Limitations of the study

Several limitations must also be acknowledged.

First, the model is a delayed variant of an existing financial system, not a completely new financial model. The novelty lies in the combined treatment of Caputo memory, a specific delayed investment-feedback term, stability diagnostics, parameter comparisons, and residual verification.

Second, only one nonlinear feedback term is delayed. This choice is useful for isolating a particular economic mechanism, but real markets may involve multiple delays, distributed delays, state-dependent delays, or delays in several feedback channels.

Third, the stability analysis for $E_{\pm}$ involves a transcendental characteristic equation. The numerical crossing criterion identifies possible first stability boundaries, but it does not provide a complete analytical classification of all characteristic roots.

Fourth, the numerical experiments focus on transient dynamics and stability tendencies. They do not constitute a complete bifurcation or chaos classification. A rigorous study of chaos would require long-time integration, Lyapunov exponents adapted to fractional delay systems, recurrence diagnostics, sensitivity analysis, and continuation in relevant parameters.

Fifth, the residual estimator is a defect measure rather than an exact error estimate. It is useful for verifying numerical consistency, but it cannot replace a complete convergence theorem for the nonlinear fractional delay problem.

These limitations define the appropriate scope of the paper. The work should therefore be read as a stability-oriented and residual-verified numerical study of memory and delayed investment response in a fractional financial model.

6.9. Reproducibility and code availability

The source codes used to produce the numerical simulations, parameter sweeps, residual diagnostics, stability scan, tables, and figures are provided as supplementary material. The supplementary files include the PECE solver for the Caputo fractional delay system, the delay interpolation routines, the quintic Caputo residual postprocessor, and the scripts used to generate the figures reported in the manuscript.

This code availability is important for reproducibility. It allows the reader to verify the baseline computation, repeat the mesh-refinement test, reproduce the memory-order and delay sweeps, and explore additional parameter values. It also makes clear which numerical evidence supports the claims made in the paper.

7. Conclusions and future work

This paper investigated a delayed Caputo fractional variant of the Chen financial system as a model for memory and delayed investment response in nonlinear economic dynamics. The model describes the interaction among the interest rate, investment demand, and price index by means of a three-dimensional fractional delay system. The delay was introduced only in the nonlinear squared-interest-rate feedback term of the investment equation. This choice reflects the idea that investment demand does not react instantaneously to past borrowing conditions, while preserving a transparent structure in which the role of a single delayed feedback mechanism can be isolated.

The equilibrium structure was obtained explicitly. The equilibrium

$$E_0 = \left(0, \frac{1}{b}, 0\right)$$

exists for all positive values of the parameters a, b, and c, whereas the two nontrivial equilibria $E_\pm$ exist under the condition

$$1 - ab - \frac{b}{c} > 0.$$

The equilibrium coordinates are independent of the delay parameter because, at a constant state, the delayed variable coincides with the present variable. Thus, the delay affects the perturbation dynamics and local stability, not the algebraic location of the equilibria.

The local stability analysis showed two different situations. At E_0, the delay disappears from the linearized system because the coefficient multiplying the delayed perturbation is proportional to x^*, which is zero at this equilibrium. A corrected characteristic equation was derived, and the fractional stability criterion was expressed in terms of the spectral values $\mu_1 = -b$ and $\mu_\pm$. For the nontrivial equilibria $E_\pm$, the delay enters the characteristic equation explicitly through the exponential factor $e^{-\lambda\tau}$. A numerical modulus–phase crossing criterion was then used to identify possible delay-dependent stability changes.

The numerical experiments were organized to separate the effects of memory and delay. The fractional-order sweep showed that changing ρ modifies the amplitude, timing, and persistence of the transient investment response. Smaller values of ρ strengthen the memory effect and tend to smooth the transient dynamics. The delay sweep showed that increasing τ can shift and amplify the investment-demand excursion, even though the equilibria remain unchanged. The direct comparison between delayed and nondelayed dynamics confirmed that the lagged nonlinear feedback modifies the finite-time adjustment process. The comparison between the fractional and integer-order responses showed that even a fractional order close to one can alter the transient amplitude, phase, and relaxation.

The phase portraits were interpreted conservatively as finite-time transient trajectories. They show bounded nonlinear motion and non-monotone coupling among the three financial variables, but they are not used as evidence of periodicity or chaos. This point is important because a finite-time phase curve alone cannot establish the existence of a periodic orbit, bifurcation branch, or chaotic attractor. Accordingly, the study is presented as a stability- oriented and residual-verified numerical analysis, not as a complete bifurcation or chaos classification.

A residual diagnostic based on an independent quintic Caputo reconstruction was included to assess numerical consistency. The residual operator was derived from local quintic interpolation and exact integration of the weakly singular Caputo kernel moments. The residual analysis showed that the largest defect occurs during the transient interval where the delayed nonlinear investment feedback is most active. Moreover, the full-mesh residual maxima decrease systematically under refinement from h to $h/2$ and $h/4$. This confirms that the residual peak is not an artifact of sparse sampling and that the computed transient response becomes more consistent as the temporal resolution is increased.

The main contribution of the paper is therefore the combination of four elements: an interpretable delayed fractional financial model, explicit equilibrium and local stability analysis, parameter comparisons separating memory and delay effects, and full-mesh residual verification. This combination provides a reproducible framework for studying delayed fractional financial systems without overstating the numerical evidence.

Several directions remain open for future work. A complete nonlinear bifurcation analysis should be carried out by continuing stability switches and constructing two-parameter diagrams in the (ρ, τ)-plane. The detection of chaotic regimes should be supported by long-time simulations, Lyapunov exponents adapted to fractional delay systems, recurrence diagnostics, and robust sensitivity tests. It would also be useful to examine alternative delay placements, multiple or distributed delays, state-dependent lags, and parameter-estimation strategies based on empirical financial data. Finally, control and synchronization methods could be developed to suppress undesirable investment oscillations or to stabilize selected equilibrium regimes.

Author contributions

Alvaro H. Salas, Gilder Cieza Altamirano and Lorenzo Julio Martínez Hernández: Conceptualization, Methodology, Validation, Writing-original draft, Writing-review & editing. All authors contributed to the development of the model, analysis of the results, and preparation of the manuscript.

Use of Generative-AI tools declaration

The authors declare they have not used Artificial Intelligence (AI) tools in the creation of this article.

Conflict of interest

The authors declare that they have no conflicts of interest.

References

1. J. H. Ma, Y. S. Chen, Study for the bifurcation topological structure and the global complicated character of a kind of nonlinear finance system (I), *Appl. Math. Mech.*, **22** (2001), 1240–1251. https://doi.org/10.1007/BF02437847
2. R. Shone, *An introduction to economic dynamics*, Cambridge: Cambridge University Press, 2012. https://doi.org/10.1017/CBO9781139164733
3. M. Jusup, P. Holme, K. Kanazawa, M. Takayasu, I. Romić, Z. Wang, et al., Social physics, *Physics Reports*, **948** (2022), 1–148. https://doi.org/10.1016/j.physrep.2021.10.005

4. V. E. Tarasov, On history of mathematical economics: application of fractional calculus, *Mathematics*, **7** (2019), 509. https://doi.org/10.3390/math7060509
5. W. C. Chen, Nonlinear dynamics and chaos in a fractional-order financial system, *Chaos Soliton. Fract.*, **36** (2008), 1305–1314. https://doi.org/10.1016/j.chaos.2006.07.051
6. W. C. Chen, Dynamics and control of a financial system with time-delayed feedbacks, *Chaos Soliton. Fract.*, **37** (2008), 1198–1207. https://doi.org/10.1016/j.chaos.2006.10.016
7. Q. Gao, J. Ma, Chaos and Hopf bifurcation of a finance system, *Nonlinear Dyn.*, **58** (2009), 209–216. https://doi.org/10.1007/s11071-009-9472-5
8. Z. Wang, X. Huang, G. Shi, Analysis of nonlinear dynamics and chaos in a fractional order financial system with time delay, *Comput. Math. Appl.*, **62** (2011), 1531–1539. https://doi.org/10.1016/j.camwa.2011.04.057
9. C. Huang, L. Cai, J. Cao, Linear control for synchronization of a fractional-order time-delayed chaotic financial system, *Chaos Soliton. Fract.*, **113** (2018), 326–332. https://doi.org/10.1016/j.chaos.2018.05.022
10. S. Wang, S. He, A. Yousefpour, H. Jahanshahi, R. Repnik, M. Perc, Chaos and complexity in a fractional-order financial system with time delays, *Chaos Soliton. Fract.*, **131** (2020), 109521. https://doi.org/10.1016/j.chaos.2019.109521
11. K. Rajagopal, F. Parastesh, H. R. Abdolmohammadi, S. Jafari, M. Perc, E. Klemenčič, Effects of coupling on extremely multistable fractional-order systems, *Chinese J. Phys.*, **87** (2024), 246–255. https://doi.org/10.1016/j.cjph.2023.12.011
12. I. Podlubny, *Fractional differential equations: an introduction to fractional derivatives, fractional differential equations, to methods of their solution and some of their applications*, San Diego: Academic Press, 1999.
13. A. A. Kilbas, H. M. Srivastava, J. J. Trujillo, *Theory and applications of fractional differential equations*, Amsterdam: Elsevier, 2006.
14. K. Diethelm, *The analysis of fractional differential equations: an application-oriented exposition using differential operators of Caputo type*, Berlin: Springer, 2010. https://doi.org/10.1007/978-3-642-14574-2
15. C. Li, W. Deng, Remarks on fractional derivatives, *Appl. Math. Comput.*, **187** (2007), 777–784. https://doi.org/10.1016/j.amc.2006.08.163
16. K. Diethelm, N. J. Ford, A. D. Freed, A predictor-corrector approach for the numerical solution of fractional differential equations, *Nonlinear Dyn.*, **29** (2002), 3–22. https://doi.org/10.1023/A:1016592219341
17. K. Diethelm, N. J. Ford, A. D. Freed, Detailed error analysis for a fractional Adams method, *Numer. Algorithms*, **36** (2004), 31–52. https://doi.org/10.1023/B:NUMA.0000027736.85078.be
18. S. Bhalekar, V. Daftardar-Gejji, A predictor-corrector scheme for solving nonlinear delay differential equations of fractional order, *J. Fract. Calc. Appl.*, **1** (2011), 1–9.